MODELING OF ION CYCLOTRON WAVES ABSORPTION IN VASIMR

Andrew V. Ilin[1], Franklin R. Chang Díaz[2], Boris N. Breizman[3], Mark D. Carter[4]

[1]Muñiz Engineering, Inc., Advanced Space Propulsion Laboratory,
NASA Johnson Space Center, Houston, Texas, 77059 USA (ilin@jsc.nasa.gov)
[2]Advanced Space Propulsion Laboratory, NASA Johnson Space Center, Houston, Texas, USA
[3]University of Texas at Austin, Austin, Texas, USA
[4]Oak Ridge National Laboratory, Oak Ridge, Tennessee, USA

ABSTRACT

The Variable Specific Impulse Magnetoplasma Rocket (VASIMR)[1,2] is potentially among the most advanced electric propulsion technologies, since it allows thrust with very high continuous variable specific impulse. Since 1995, the Advanced Space Propulsion Laboratory at the NASA Johnson Space Center has conducted experimental and theoretical research on the VASIMR. Ion cyclotron resonant heating (ICRH) is the main mechanism of power deposition from radio waves, generated by the Ion Cyclotron Radio Frequency (ICRF) antenna, into the VASIMR plasma (Figure 1). The goal of numerical simulations is to model the underlying physics processes and to help design a Radio Frequency (RF) antenna to maximize heating efficiency. There are also two closely related tasks: to model the magnetic nozzle and to optimize the overall performance of VASIMR[3]. Mathematical simulation of ICRH helps to design an RF-antenna, i.e. make maximal absorption of RF power into the plasma in the resonance area.

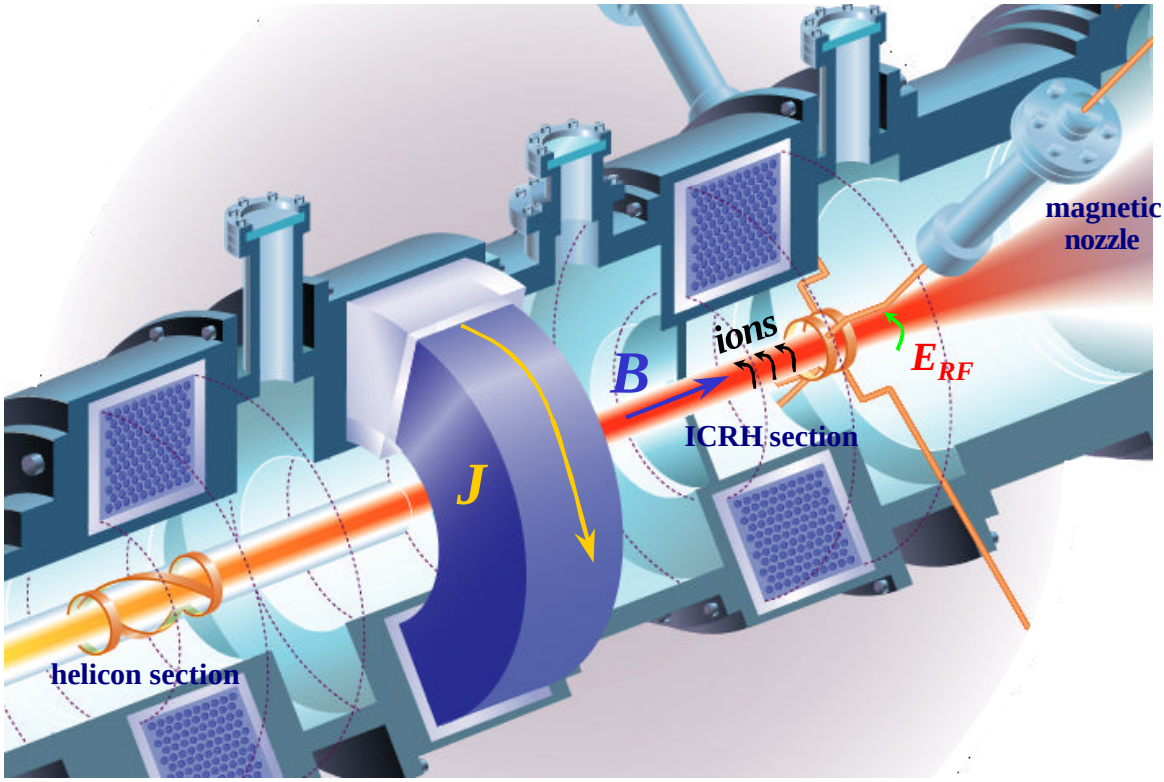

Figure 1. Ion Cyclotron Resonance Heating section in VASIMR (in the middle). Rotating electric field at the frequency corresponding the ion gyro frequency accelerates the ion spiral motion. At left, the helicon antenna is shown for the plasma generation. At right, the magnetic nozzle serves the purpose of the conversion of the spiral motion of ion into directed axial motion.

MATHEMATICAL MODEL

In the EMIR code[4], the RF electric field, $\boldsymbol{E}_{RF}$, magnetic field, $\boldsymbol{B}_{RF}$, and RF antenna current density, $\boldsymbol{j}_{RF}$, are expanded in a periodic Fourier sum in the azimuthal coordinate to reduce the three-dimensional problem to a weighted sum over two-dimensional solutions. Implicit time dependence is assumed as well as azimuthal symmetry of the equilibrium quantities, so that the fields and currents can be expanded into azimuthal modes:

$$\boldsymbol{E}_{RF}(r,f,z,t)=\sum_m \boldsymbol{E}_m(r,z)e^{imf-iwt}\,, \tag{1}$$

where m is an azimuthal mode number and w is RF frequency.

The RF fields are obtained by solving Maxwell's equations, written in harmonic form:

$$\nabla\times\left(\frac{\boldsymbol{B}_{RF}}{m}\right)=-iwe\boldsymbol{E}_{RF}+\boldsymbol{j}_p+\boldsymbol{j}_{ANT}\,, \tag{2}$$

$$\nabla\times\boldsymbol{E}_{RF}=iw\boldsymbol{B}_{RF}\,. \tag{3}$$

Substitution of the $\boldsymbol{B}_{RF}$ from (3) into the (2) leads to the following wave equation for $\boldsymbol{E}_{RF}$:

$$-\nabla\times\nabla\times\boldsymbol{E}_{RF}+\frac{w^2}{c^2}(\boldsymbol{E}_{RF}+\frac{i}{we}\boldsymbol{j}_p)=-iwm\boldsymbol{j}_{ANT}\,. \tag{4}$$

In the current EMIR implementation, the plasma current density $\boldsymbol{j}_P$ is related to the electric field by a collisional cold plasma conductivity tensor $\boldsymbol{j}_p=\hat{s}\cdot\boldsymbol{E}_{RF}$ with collisional de-correlation. Equation (4) can then be represented by system of independent equations with respect to $\boldsymbol{E}_m$ as suggested by Stix[5]:

$$-e^{-imf}\nabla\times\nabla\times\boldsymbol{E}_m e^{imf}+\frac{w^2}{c^2}\hat{\boldsymbol{K}}\cdot\boldsymbol{E}_m=-iwm\boldsymbol{j}_m\,, \tag{5}$$

where $\hat{\boldsymbol{K}}=\boldsymbol{I}+\frac{i}{we}\hat{\boldsymbol{s}}$ is a cold plasma dielectric tensor:

$$\hat{\boldsymbol{K}}=\begin{pmatrix}K_\perp & -iK_x & 0\\ iK_x & K_\perp & 0\\ 0 & 0 & K_{||}\end{pmatrix}, \tag{6}$$

and $\boldsymbol{j}_m$ is the current density externally applied by an antenna. The entries of the dielectric tensor depend on the plasma density n_i and the vacuum magnetic field B_0 and the driven frequency w for a multiple-ion plasma as follows:

$$K_\perp=1-\sum_{l=e,i}\frac{w_{pl}^2}{w^2-w_{cl}^2},\quad K_x=\sum_{l=e,i}\frac{w_{ci}}{w}\frac{w_{pl}^2}{w^2-w_{ci}^2},\quad K_{||}=1-\sum_{l=e,i}\frac{w_{pl}^2}{w^2},\quad w_{pl}^2=\frac{e^2n_l}{e_0\tilde{m}_l},\quad w_{cl}=\frac{eB_0}{\tilde{m}_l}\,, \tag{7}$$

where the sum is over the electrons and all ion species.

In these equations, $\boldsymbol{E}_m$ is the complex m-mode of RF electric field vector, l denotes the electron and ion plasma species, e denotes the electron charge, $\tilde{m}_l$ denotes the complex species mass, n_l denotes the species density, B_0 denotes the static magnetic field strength, m_0 and e_0 are the permeability and permittivity of free space, w is the driven RF frequency, and $\boldsymbol{j}_{ANT}$ represents RF current sources from the antenna; all units are MKS. The || subscript denote parallel component, $\perp$ and x subscripts denote perpendicular components with respect to the static magnetic field direction.

Absorption is introduced in the cold plasma model by adding an imaginary collision frequency to the RF driven frequency, which is equivalent to adding an imaginary particle mass in the dielectric tensor elements:

$$\tilde{m}_l=m_l(1+ia_l)=m_l\left(1+i\frac{n_l}{w}\right). \tag{8}$$

The considered version of the EMIR code also assumes that $w_{pe} >> w$ such that the $K_{||}$ term in the dielectric tensor is very large. This assumption leads to the condition that $E_{||}$ is very small because of the high mobility of electrons along magnetic field lines, and thus, $E_{||} = 0$ is assumed. The solution of Maxwell's equations is considerably simplified by neglecting this parallel field component (but not the parallel current) giving a relation between axial and radial components of $\boldsymbol{E}_{RF}$:

$$E_z = - B_{0z} E_r / B_{0z}. \tag{9}$$

The final system of equations for E_r and E_ϕ has the following form

$$\frac{\partial^2 rE_r}{\partial z^2} + \frac{r}{R}\frac{\partial^2 arE_r}{\partial r \partial z} + \left(\frac{w^2}{c^2}K_\perp - \frac{m^2}{r^2}\right)\frac{rE_r}{B_{0z}^2} + \frac{a}{R}\left(r\frac{\partial^2 rE_r}{\partial r \partial z} + \frac{r}{R}\frac{\partial}{\partial r}r\frac{\partial arE_r}{\partial r} + im\frac{\partial rE_f}{\partial z}\right) -$$
$$- i\frac{w^2}{c^2}\frac{K_x}{B_{0z}}rE_f - \frac{im}{r}\frac{\partial rE_f}{\partial r} = -iwmr\left(j_{r,m} - \frac{ar}{R}j_{z,m}\right), \tag{10}$$

$$r\frac{\partial}{\partial r}\left(\frac{1}{r}\frac{\partial rE_f}{\partial r}\right) + \frac{\partial^2 rE_f}{\partial z^2} + \frac{w^2}{c^2}K_\perp rE_f - \frac{im}{R}\frac{\partial arE_r}{\partial z} + i\frac{w^2}{c^2}\frac{K_x}{B_{0z}}rE_r - imr\frac{\partial}{\partial r}\left(\frac{E_r}{r}\right) = -iwmrj_{f,m}, \tag{11}$$

where $a = B_{0r}R/(B_{0z}r)$, R is the radius of a perfectly conducting wall boundary. Boundary conditions for equations (10, 11) are derived from the property, that the tangential component of $\boldsymbol{E}_m$ vanishes on the boundary $r = R$, and $z = 0, L$. This gives $E_r = E_f = 0$ at $z = 0, L$ and at $r = R$. The computational domain for equations (10, 11) is shown in Figure 2. In the discretization, Equations (10) and (11) are solved with respect to the dependent variables rE_r and rE_f.

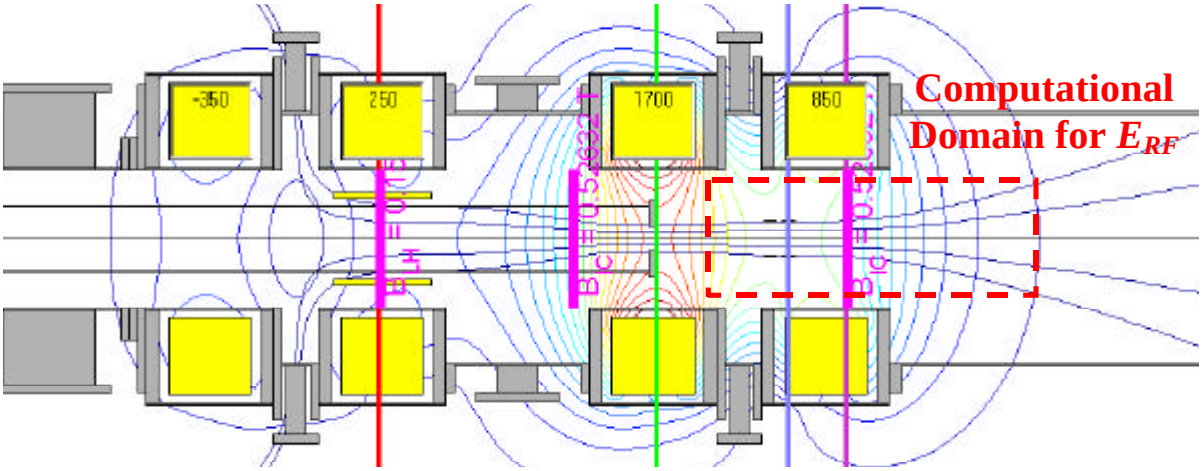

Figure 2. Computational domain for solution of the equations (10, 11) shown relatively to the overall magnetic configuration of the VX-10 experiment. Increasing domain makes computation more expensive. Reducing the domain make the solution less accurate. The pink vertical bold lines show the areas of the Ion Cyclotron 2 MHz RF waive resonance for the given electromagnet currents and using Helium as a propellant.

The RF power absorption by the plasma for a known antenna current determines the plasma loading resistance, which is a very important parameter for an antenna design. In a lumped circuit model, the resistance for each antenna segment can be defined as twice the power emitted by that segment divided by the square of the current in that segment. In order to efficiently couple RF power, the plasma loading resistance for the entire antenna must be substantially larger that the vacuum loading resistance, which is caused by finite resistance effects throughout the entire circuit driving the antenna.

In many cases, good antenna designs permit a reasonably accurate solution using just one major mode m. For more accurate calculations, several m modes are used and the system (10, 11) is solved independently for each m, and the final solution in real space is obtained by summing over the modes.

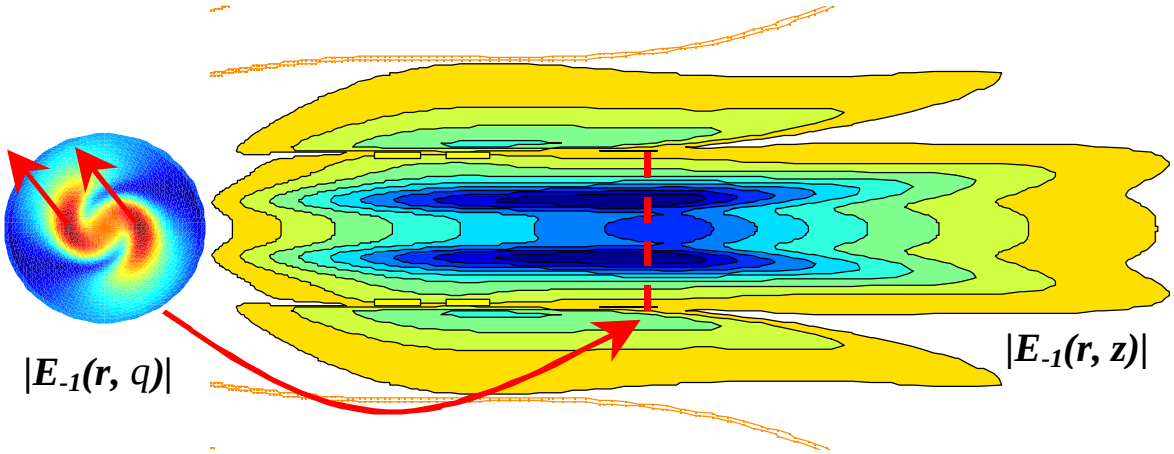

Figure 3. Contours of the electric field component having the proper polarization for ion absorption for $m = -1$. Parabolic profile of the Helium plasma was assumed with maximal density $n_i = 3\ 10^{18}\ m^{-3}$.

In Figure 3 we show the RF electric field amplitudes and absorbed power for the $m = -1$ mode ($m = 1$ for the opposite magnetic field direction) propagating from the antenna to a magnetic beach, where w is equal to the ion gyro-frequency. The $m = -1$ mode penetrates to the axis with the correct polarization to accelerate ions in the direction perpendicular to the static magnetic field. A good antenna design for the ICRF section will excite primarily the $m = -1$ mode and produce a loading resistance that is high enough for the desired power of 6-8 kW to be coupled by the RF feed system, matching network, and transmitters.

The power coupled to the plasma must equal the power emitted by the antenna according to Poynting's theorem

$$\int_V \frac{1}{2} Re[\mathbf{E}_{RF} \cdot (\mathbf{j}_p + \mathbf{j}_{ANT})^*]dV + \oint_{\partial V} Re(\mathbf{S} \cdot \mathbf{n}) d(\partial V) = 0, \qquad (12)$$

where $\mathbf{S} = (\mathbf{E}_{RF} \times \mathbf{B}_{RF}^*) / (2m_0)$ is the complex Poynting vector and $\mathbf{n}$ is the unit vector normal to the integration surface. Taking the volume of integration over the perfectly conducting boundary eliminates any contributions from the Poynting flux through the boundaries. Using the conductivity tensor to calculate the plasma current and evaluating the volume integral gives the total power absorbed by the plasma for a known antenna current. Convergence of the difference scheme can be measured by calculating the power generated by the antenna $P_{ANT} = \int_V \frac{1}{2} Re[\mathbf{E}_{RF} \cdot \mathbf{j}_{ANT}^*]dV$ and comparing it with the absorption in the plasma. In our numerical experiment we observed convergence of the relative power error, calculated by the formula: $e_P = \left|1 - \frac{P_p}{P_{ANT}}\right| \cdot 100\%$. As shown in numerical experiments, the level of $e_p < 5\%$ requires the mesh size to be larger than (600×200). To resolve big mesh problem on computers with limited memory, the efficient iterative solver can be applied[6].

To obtain a reasonably self-consistent picture, ion trajectories are followed through the static and the RF fields using the particle trajectory tracing code VASIMR[3]. The VASIMR and EMIR codes are then iterated to estimate the ICRH effects on the plasma density. The iteration is performed by calculating the RF-fields with the EMIR code, and using these fields to follow nonlinear ion trajectories with the VASIMR code on the gyro-frequency time scale. The ion trajectories are used to generate RF-power absorption values and a density input for the next EMIR calculation. The codes are iterated until the density profile converges, then the collisional absorption parameter in the EMIR code is adjusted and the iteration is continued until the power deposited by the RF-system matches the power absorbed by the ion trajectories in a global sense.

RESULTS OF MATHEMATICAL MODELING

a) Optimal plasma density regimes

VASIMR performs well, when the plasma gets heated uniformly across the radius. High plasma density makes the resistance too large and the RF field does not propagate to the plasma center. As shown in Figure 4, for plasma density higher than $3\ 10^{18}\ m^{-3}$, the central area of plasma will not be heated by RF field and VASIMR efficiency is not going to be high.

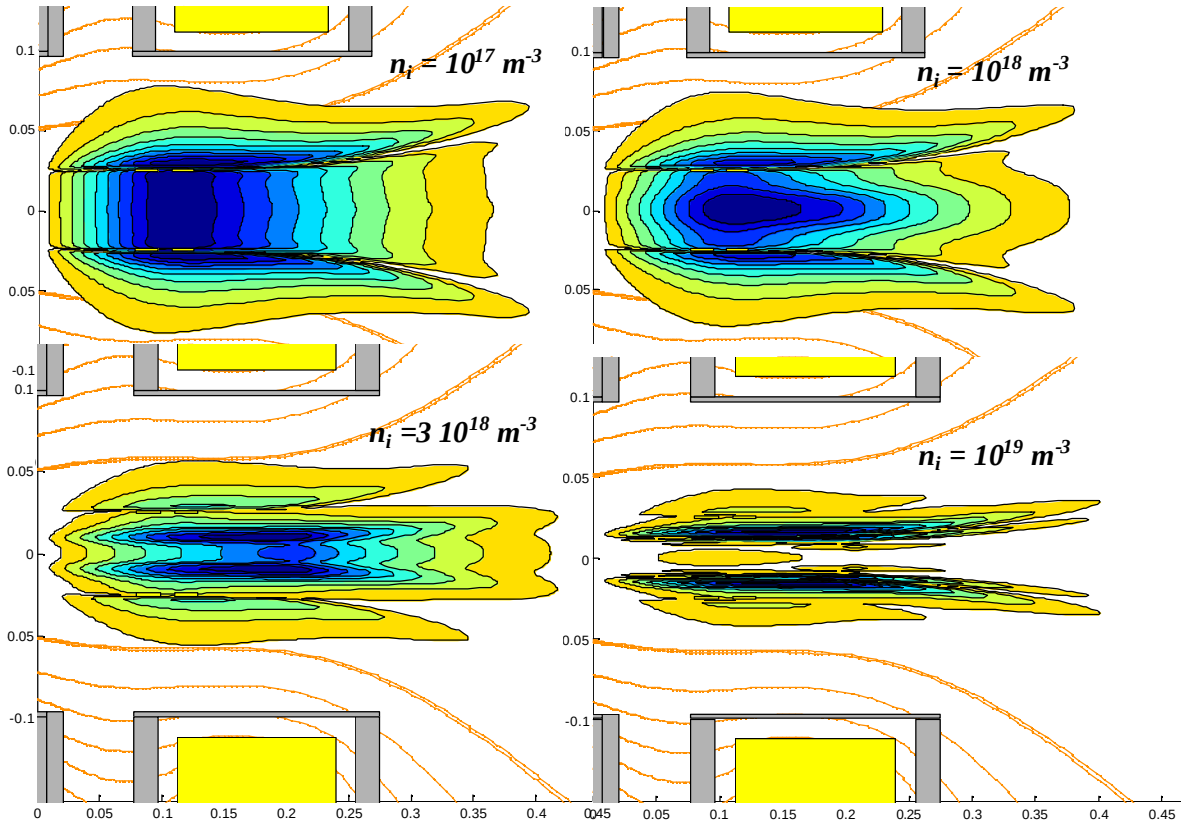

Figure 4. Comparison of the electric field components $|E_{-1}(r, z)|$ for different values of the maximal ion density $n_i = 10^{17}$ ¸ $10^{19}\ m^{-3}$.

b) Effect of the magnetic baffle.

As shown in Figure 2, VASIMR has two areas of ICRF resonance. One area is located down the plasma flow from the ICRF antenna. This is the place where most ICRF power gets absorbed into the plasma. The second area of ICRF resonance is located up the plasma flow in the plasma generation section. It is desirable to prevent ICRF wave propagation toward the second resonance area. It can be achieved by placing an RF baffle, a metal disc with a hole for the plasma path, placed in the area where magnetic field is the largest, and the plasma is most thin. As shown in Figure 5, the baffle plays his role very well. Numerical simulation demonstrates that the outer diameter of the baffle disc does not need to be large.

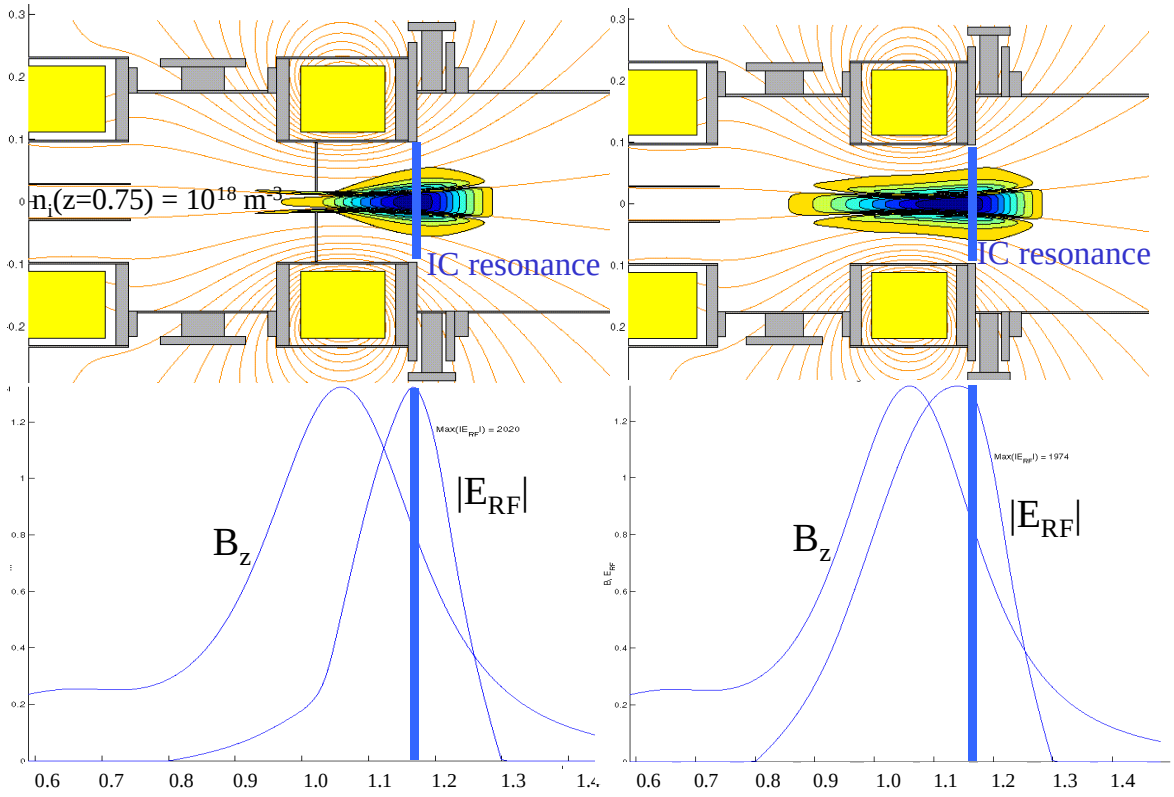

Figure 5. RF baffle (shown at left half of the figure) stops RF waves from propagating up the plasma flow toward the plasma generation area (compare to the right half of the figure). Here computational domain was shifted to the left to cover some additional area.

c) Optimal magnetic configuration design

Laboratory and numerical experiments demonstrated that ICRF heating in VASIMR works much better if the magnetic configuration has a flat area under the ICRF antenna. As shown in Figure 6, placing the antenna between the electromagnets, and choosing corresponding currents can create the flat magnetic field of desired strength under the antenna. If the flat magnetic field strength is the same as ICRF resonance field, i. e. ICRF resonance is located under the antenna, then the ICRF power absorption by plasma is not efficient (see left side of Figure 6). Numerical experiments demonstrate much higher ICRF loading in the case where the flat magnetic field under the antenna is about 10% higher than ICRF resonance field, and resonance is located about 10 cm down the plasma flow from the antenna (see right side of Figure 6).

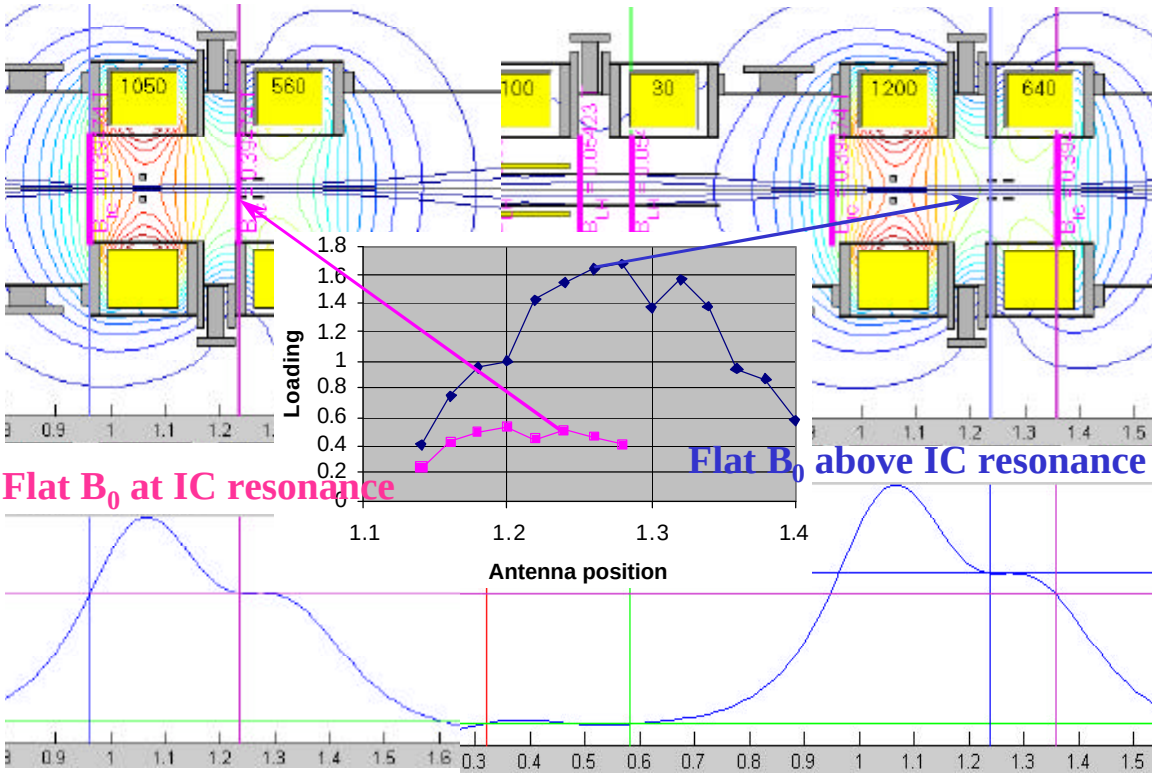

Figure 6. ICRF loading is plotted as a function of the antenna position (center part). Left side of the Figure demonstrates magnetic configuration, when flat magnetic field is the same as resonance field. Right side of the Figure demonstrates the configuration, when the flat magnetic field is 10% higher than the resonance field. Upper plots show two-dimensional configuration, bottom half of the figure shows one-dimensional plots of the magnetic field strength.

MODEL DEVELOPMENT

Linear description of the plasma response near the resonance is the most sensitive part of the present modeling. This is related to the fact that the ions gain their total energy in a single pass through the resonance. A recently developed nonlinear resonance model[7] offers a fully consistent way of calculating the ion current in the plasma. The improved technique can be implemented by either particle or fluid approach. Additional work is needed to demonstrate the effect of nonlinear resonance and compare results with those obtained within the previous linear assumptions.

NOMENCLATURE

$\boldsymbol{B}$	magnetic induction ($0 - 1$ Tesla)
c	speed of light ($3\ 10^8$ m / s)
$\boldsymbol{E}$	electric field (Volt / m)
e	electron charge ($1.6\ 10^{-19}$ Coulomb)
$\boldsymbol{I}$	identity tensor
i	imaginary unit
$\boldsymbol{j}$	current density ($0 - 10^5$ Ampere / m^2)
$\boldsymbol{K}$	dialectric tensor
L	length of the domain (0.5 m)
m	azimuthal mode number
m_l	particle mass (kg)
n	plasma particle density ($0 - 10^{19}$ m^{-3})
$\boldsymbol{n}$	normal vector
P	power ($24{,}000$ Watt)
r, f, z	cylindrical coordinates: radial (m), azimuthal (rad) and axial (m)
R	radius of the wall (0.2 m)
$\boldsymbol{S}$	Poynting vector
t	time (s)
V	computational domain
a	parameter in (10, 11)
a_l	collisional parameter in (8)
e	electric permittivity ($8.85\ 10^{-12}$ F / m)
m	magnetic permeability ($1.25\ 10^{-6}$ Henry / m)
n_l	collision frequency (s^{-1})
s	plasma conductivity tensor
w	RF frequency (rad / s)

Subscripts:

0	vacuum, inlet
ANT	ICRF antenna
e	electron
i	ion
l	particle
p	plasma
RF	radio frequency
$\wedge, x$	orthogonal directions to vacuum magnetic field $\boldsymbol{B_0}$
$\parallel$	parallel to vacuum magnetic field $\boldsymbol{B_0}$

ACKNOWLEDGMENTS

This research was sponsored by NASA Johnson Space Center.

REFERENCES

1. Chang Díaz F.R., "Research Status of The Variable Specific Impulse Magnetoplasma Rocket", *Proc. 39th Annual Meeting of the Div. of Plasma Physics* (Pittsburgh, PA, 1997), *Bulletin of APS*, **42** 2057.

2. Chang Díaz, F. R., "VASIMR engine", *The Scientific American*, **283** (2000) 72-79.

3. Ilin A.V., Chang Díaz F.R., Squire J.P. and Carter M.D. "Monte Carlo Particle Dynamics in a Variable Specific Impulse Magnetoplasma Rocket", (*Proceedings of Open Systems' 98), Transactions of Fusion Technology,* **35** (1999) 330 – 334.

4. Jaeger E.F., Batchelor D.B., Weitzner H. and Whealton J.H. "ICRF Wave Propagation And Absorption in Tokamak And Mirror Magnetic Fields – A Full-wave Calculation", *Computer Physics Com*., **40** (1986) 33 – 64.

5. Stix T. H. "Waves in Plasmas", American Institute of Physics, New York, (1992).

6. Ilin, A. V., Chang Díaz, F. R., Squire, J. P., and Carter, M. D., "Radio Frequency Field Calculations for Plasma Heating Simulations in VASIMR", *Proceedings of 53th International Astronautical Congress' October 10-19, 2002*, Houston, TX, IAC-02-S.P.07 (2002) 6.

7. Breizman B. N., Arefiev A. V., "Single-pass ion cyclotron resonance absorption", *Physics of Plasmas*, **8** (2001) 907-915.